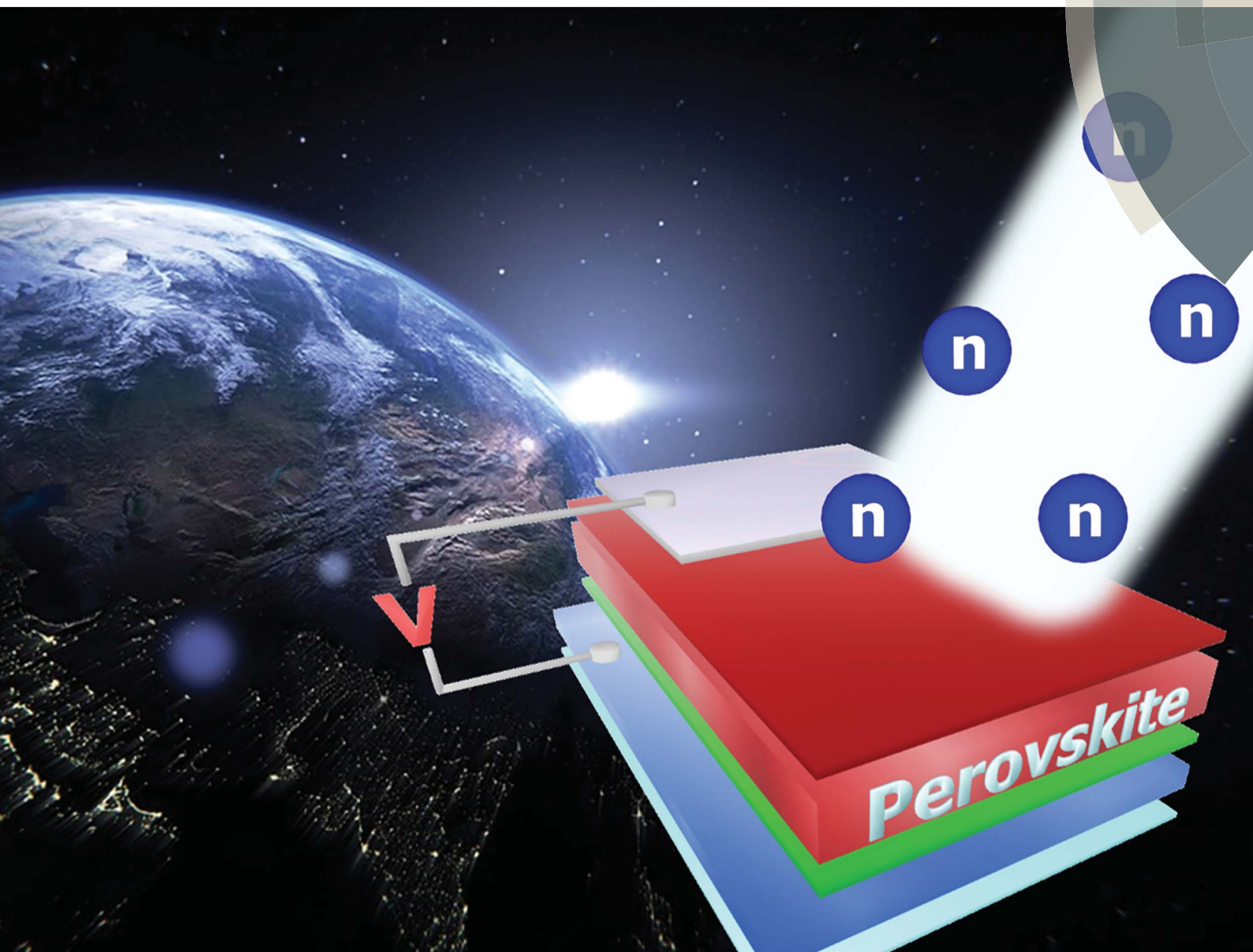


Sustainable Energy & Fuels

Interdisciplinary research for the development of sustainable energy technologies

rsc.li/sustainable-energy



ISSN 2398-4902



ROYAL SOCIETY
OF CHEMISTRY

Celebrating
IYPT 2019

COMMUNICATION

V. Garcia Sakai, F. Cacialli *et al.*

Perovskite solar cell resilience to fast neutrons



Perovskite solar cell resilience to fast neutrons

Cite this: *Sustainable Energy Fuels*,
2019, 3, 2561G. M. Paternò,^{†a} V. Robbiano,^a L. Santarelli,^a A. Zampetti,^{†a} C. Cazzaniga,^b
V. Garcia Sakai^{†b*} and F. Cacialli^{†a*}Received 19th February 2019
Accepted 25th April 2019

DOI: 10.1039/c9se00102f

rsc.li/sustainable-energy

The high power-per-weight ratio displayed by metal-halide perovskite solar cells is a key advantage of these promising devices for applications that require low payload, such as in space and avionics. However, little is known about the effect of the outer space radiation environment on these devices. Here, we report the first *in operando* study on fast neutron irradiation of perovskite solar cells. We show the remarkable resilience of these devices against one of the most hazardous forms of radiation that can be found at flight altitude and in space. In particular, our results highlight a comparable *in operando* degradation pattern between light soaked and light + neutron irradiated devices. However, whereas light-induced degradation is fully reversible, fast neutrons lead to permanent effects likely originating from atomic displacement in the active material. We also propose that such irreversible worsening is alleviated by the formation of neutron-induced shallow traps, which act as dopants and contribute to the increase of open circuit voltage and the decrease of leakage current in light + neutron irradiated devices. The high radiation dose that perovskite-based solar cells can potentially withstand renders these devices highly appealing for space and avionic applications.

Introduction

Metal-halide perovskites have emerged in recent years as excellent photovoltaic (PV) materials, owing to their relatively high extinction coefficient (10^5 cm^{-1}), broadband absorption, high charge mobility and diffusion length, as well as easy processability from solution.^{1,2} Taken together, these properties allow the fabrication of low-cost, lightweight and efficient devices that exhibit a high power-per-weight ratio (23 W g^{-1}),³ a parameter that represents an important figure of merit to

assess the possible application of PV diodes in avionics and space missions.⁴ Furthermore, the compatibility of perovskite-based PV technology for scalable printing deposition techniques, such as roll-to-roll or ink-jet printing, can enable full fabrication of photovoltaic modules *in situ* i.e. during long-duration space travels.⁵ The harsh radiation environment in space, however, can pose severe degradation hazards to such rather defective materials,^{6–8} practically preventing perovskite solar cells from entering the space industry. Therefore, a detailed understanding of the effect of outer space radiation on perovskite PV performance is highly desirable.

Within this context, a number of research groups have started investigating the interaction between highly energetic particles present in cosmic-rays (i.e. protons and electrons) and perovskites, to understand the possible degradation pathways experienced by these materials in a low earth orbit and space.^{9–13} From a quantitative point of view, in these experiments the authors usually irradiate their devices with a particle flux of 10^{12} – 10^{15} cm^{-2} mimicking days of proton irradiation in outer space or years in a low earth orbit, observing little (5–6%) or no efficiency decrease after such an irradiation protocol. Therefore, all these studies point towards the remarkable radiation tolerance of perovskite PVs which is even superior to that of crystalline silicon devices (i.e. 3 orders of magnitude higher for proton irradiation).¹¹ Such a feature has been related to the self-healing properties of the mixed covalent-ionic perovskite lattice, which allows self-passivation of the radiation-induced defects.¹¹ However, to date there are no studies on the radiation tolerance of perovskite materials upon irradiation by (so-called) “fast neutrons” (i.e. with an energy $>10 \text{ MeV}$), which in fact represent one of the most severe forms of radiation at aircraft altitudes, in avionic and space environments.¹⁴ Fast neutrons are secondary particles generated upon interaction of primary cosmic-rays ($\sim 90\%$ protons) with the atmosphere and air/spacecraft shielding and components,^{15,16} causing atomic displacements and leading to both irreversible and reversible “soft-errors” in electronic devices at the sea^{17,18} and flight level.¹⁹ For instance, it has been calculated that the International Space Station (ISS)

^aDepartment of Physics and Astronomy, London Centre for Nanotechnology, University College London, London, WC1E 6BT, UK. E-mail: f.cacialli@ucl.ac.uk^bISIS Pulsed Neutron and Muon Source, Science and Technology Facilities Council, Rutherford Appleton Laboratory, Harwell Science and Innovation Campus, Didcot, OX11 0QX, UK. E-mail: victoria.garcia-sakai@stfc.ac.uk[†] Present address. Center for Nanoscience and Technology, Istituto Italiano di Tecnologia, Milan, 20133, Italy.

receives a fluence of $\sim 2.8 \times 10^{11}$ neutrons cm^{-2} per year, in a wide energy range (10^{-1} – 10^{11} eV), featuring a broad tail in the fast neutron region (Fig. 1).¹⁴ For these reasons, neutrons are not only employed for gaining spectroscopic and structural information,^{20,21} but also for assessing the resilience of electronics in harsh radiation environments.^{22,23}

Here, we extend our previous studies on neutron irradiation of organic electronics²³ to perovskite-based PVs. The analysis of the electric PV characteristics either under light illumination (control device) or upon the combined action of light and fast neutrons highlights the irreversible nature of the neutron-induced effects, in stark contrast with the fully reversible photoinduced degradation. We propose that the formation of irreversible defects is promoted mostly by fast neutron-induced atomic displacement in the active layer.

Materials and methods

Neutron irradiation

The VESUVIO beamline^{24,25} at the ISIS spallation neutron source is well-suited for carrying out accelerated neutron radiation hardening tests,²⁶ as it is able to mimic years of neutron exposure in space in a few hours. In addition, the spallation process underpinning neutron production at ISIS is somewhat similar to what happens in space, relying on the spallation reactions induced by 800 MeV primary proton bunches accelerated in a synchrotron and colliding on a tungsten target. Therefore, the fast neutron spectrum from ISIS closely resembles the one in space and planetary environments, but with a much higher intensity (at least six orders of magnitude compared with the ISS fast neutron spectrum, see Fig. 1).²³ At a normal primary proton current ($180 \mu\text{A h}^{-1}$) the integrated fast neutron (>10 MeV) flux was determined²⁶ to be approximately $6 \times 10^4 \text{ n cm}^{-2} \text{ s}^{-1}$ whereas the estimated fast neutron fluence received by the ISS is $\approx 0.6 \text{ n cm}^{-2} \text{ s}^{-1}$ (Fig. 1),¹⁴ meaning that 1 h of irradiation corresponds to ≈ 10 years of exposure on the ISS. We irradiated our devices for up to 435 min ($1.5 \times 10^9 \text{ n cm}^{-2} \text{ s}^{-1}$) mimicking approximately 80 years of fast neutron exposure on the ISS.

Solar cell fabrication and characterisation

For the *in-operando* measurements, we recorded the current vs. voltage (I – V) characteristics every 15 min up to 435 min, either under light illumination with a calibrated halogen lamp (80 mW cm^{-2} , calibrated against a reference silicon cell) or under light + neutron irradiation. The cells were also characterized before and after light/neutron irradiation to evaluate possible reversibility of the radiation-induced effects, by using a Class A solar simulator (ABET Technologies) at AM 1.5G and 100 mW cm^{-2} . The cells after light soaking and neutron irradiation were measured one week after the experiment, to allow for radioactive decay in order to handle the cells. To minimize hysteretic behavior,²⁷ we fabricated inverted solar cell structures^{11,12,28} (Fig. 2) following a fabrication procedure used in previous experiments,^{29,30} and deposited the perovskite layer by employing a deposition procedure recommended by the material supplier (Ossila Ltd.).³¹ Finally, the cells were encapsulated with a glass slide to minimize degradation due to environmental oxygen/moisture. The average power conversion efficiency (PCE) of the devices (six samples) was $6 \pm 1\%$, a value that is below the current state-of-the-art inverted perovskite PV diodes ($\approx 12\%$).

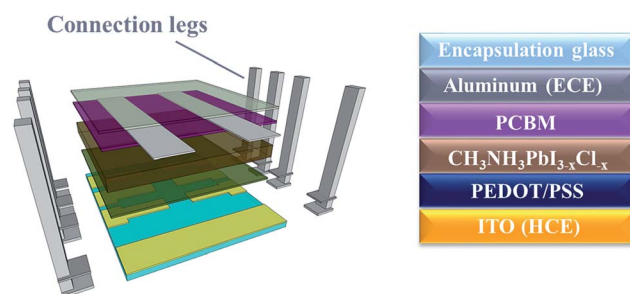


Fig. 2 Schematic representation of the fabricated solar cells, with a layer sequence of (bottom to top) glass/ITO/PEDOT:PSS/ $\text{CH}_3\text{NH}_3\text{PbI}_{3-x}\text{Cl}_x$ /PCBM/Al, where ITO is indium tin oxide, PEDOT:PSS is poly(3,4-ethylenedioxythiophene) polystyrene sulfonate and PCBM is [6,6]-phenyl-C61-butyric acid methyl ester. ECE stands for electron-collecting electrode and HCE for hole-collecting electrode.

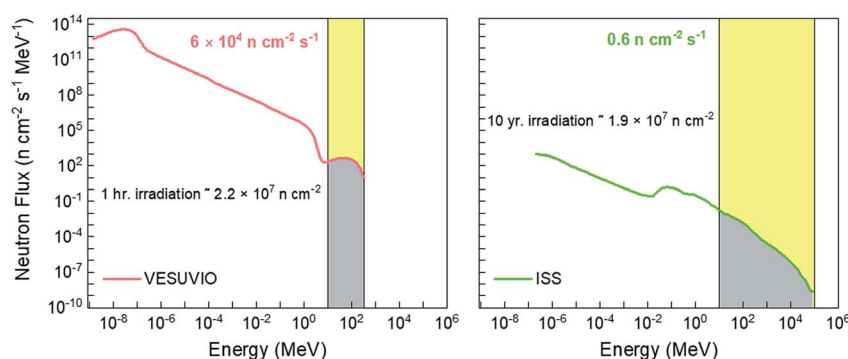


Fig. 1 Neutron energy spectrum measured using the VESUVIO beamline²⁴ (left) and the estimated flux on the ISS¹⁴ (right). Adapted from Fig. 3 of ref. 14 (T. W. Armstrong and B. L. Colborn, Predictions of secondary neutrons and their importance to radiation effects inside the International Space Station, *Radiat. Meas.*, 2001, **33**, 229–234, DOI: 10.1016/S1350-4487(0000152-9)), and from Fig. 4 of ref. 24 (R. Bedogni, *et al.*, Characterization of the neutron field at the ISIS-VESUVIO facility by means of a Bonner sphere spectrometer, *Nucl. Instrum. Methods Phys. Res., Sect. A*, 2009, **612**, 143–148, DOI: 10.1016/j.nima.2009.09.004). The yellow/grey areas indicate the fast neutron spectral component.



This can be attributed to the non-optimized fabrication procedure that did not involve the use of calcium as an electron-collecting electrode (in terms of work function),³¹ since in preliminary studies³² we observed complete degradation of PV characteristics under neutron irradiation probably due to neutron activation of calcium.³³

Results and discussion

Fig. 3(a and b) shows the I - V characteristics under light illumination (a) and light + neutron irradiation (b). In general, it is possible to discern a progressive decrease of the current, while the open circuit voltage (V_{oc}) features a slight yet noticeable increase that is much clearer in neutron irradiated devices than light-soaked devices. If we look at the PV parameters as extracted from the *in-operando* measurements (Fig. 2(a and b)), we observe a degradation pattern that is comparable between the light and light + neutron irradiated devices, with the short circuit current (J_{sc}) mostly driving the loss in efficiency of the PV diodes. However, it is worth noting some subtle yet important differences between the two sets of measurements namely (i) a more pronounced increase of V_{oc} for light + neutron irradiated (6%) devices than for light soaked (2%) devices which, however, lies within the standard deviation ($\pm 5\%$); (ii) a more substantial loss in J_{sc} , FF and, thus, the PCE for the light soaked (PCE loss = 60%) cells than that observed for light + neutron irradiated cells (PCE loss = 45%). Hence, this suggests that although the *in operando* behaviour is qualitatively identical, neutrons seem to trigger a different degradation pathway. Therefore, to obtain

a quantitative insight into this behavior we analyzed the cells' characteristics by means of the one-diode equation (eqn (1)).^{29,34,35}

$$I(V) = I_{\text{photo}} - I_0 \exp \left[\frac{q(V + IR_s)}{nk_b T} - 1 \right] - \frac{V + IR_s}{R_{\text{sh}}} \quad (1)$$

where I is the current measured at the cell electrodes, V is the voltage measured across the cell, I_{photo} is the photogenerated current, I_0 is the reverse saturation current density (leakage current), q is the elementary charge, R_s is the series resistance, R_{sh} is the shunt resistance, k_B is the Boltzmann constant, T is the absolute temperature, and n is the ideality factor. In particular, we focused our attention on three main parameters: I_0 is an equilibrium charge recombination parameter;³⁶ R_s represents the resistance experienced by each charge from generation to collection and strongly depends on the contact resistance between the active layer and the electrodes and on the charge mobility across the material; and R_{sh} is related to the presence of alternative current paths (shunts) for the light-generated current. A high leakage current usually indicates a high rate of recombination, whereas a high R_s denotes poor mobility and/or collection at the electrodes. A low R_{sh} implies the presence of shunts, *i.e.* at the grain boundaries or at the interfaces. I_0 shows a general increase upon light soaking (70% at 435 min of irradiation) and light/neutron irradiation (60%). The increase of the leakage current signifies the formation of recombination centers, and it has been related to the presence of spatially localized deep-level traps with a polaronic character due to either localized lattice strain³⁷ or photoinduced

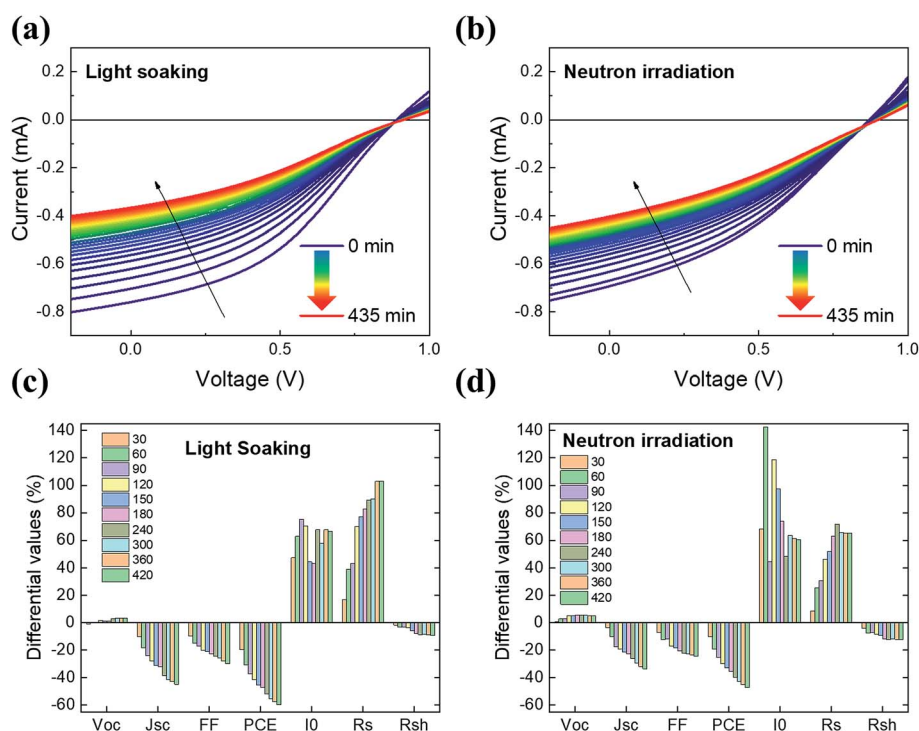


Fig. 3 (a) Evolution of the I - V characteristics under prolonged light-soaking and (b) light/neutron irradiation. We took one measurement every 15 min up to 435 min. The curves represent an average of three devices, with a standard deviation of $\approx 5\%$. (c) Evolution of the PV parameters under light soaking and (d) light/neutron irradiation.



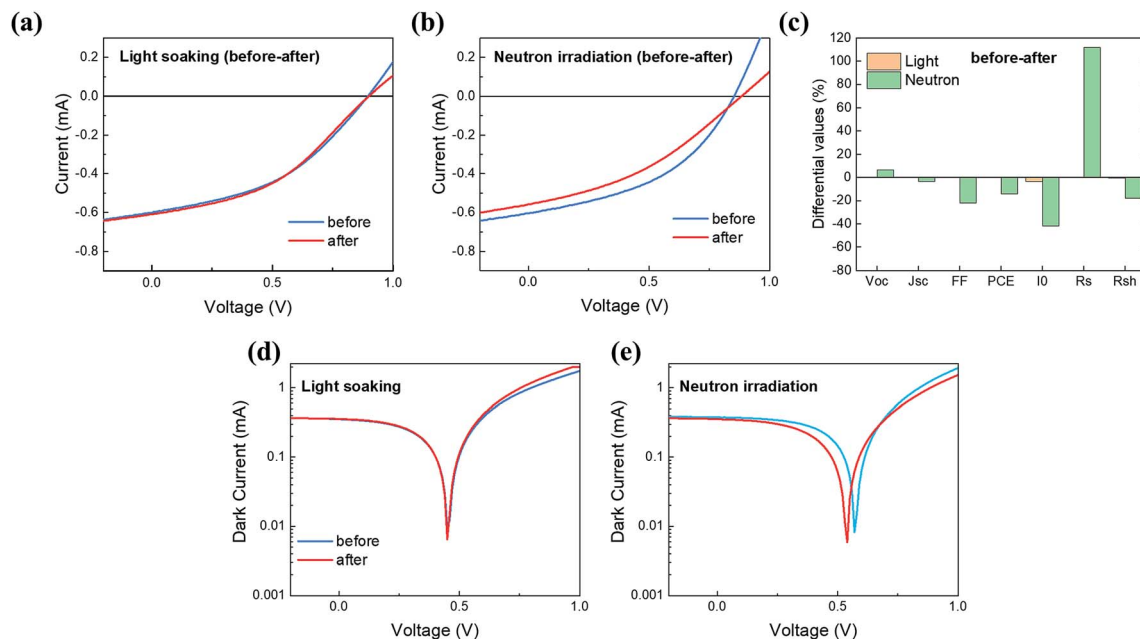


Fig. 4 (a) I - V characteristics before and after light soaking and (b) light/neutron irradiation. (c) Device parameters under the same conditions. (d) Semi-logarithmic plot of the dark current before and after light soaking and (e) light/neutron irradiation. The measurements after light and light/neutron irradiation were taken after one week, to permit complete radioactive decay due to neutron activation. The standard deviation of the device parameters is $\approx 5\%$.

deprotonation and dissociation of methylammonium molecules.^{9,12} The concomitant increase of R_s and the decrease of R_{sh} point towards the formation of traps located in the active layer and at the electrodes for both light and neutron irradiated cells, even though R_s presents a more substantial increase upon light soaking (100%) than upon light/neutron exposure (65%). This again suggests the occurrence of a competitive neutron-induced process that tends to compensate the effects generated by light illumination only. To distinguish between the reversible light-activated effects and neutron induced degradation it is therefore important to compare the device characteristics before and after light and neutron exposure, since it has been demonstrated that light-induced effects are in general reversible.³⁷

The I - V curves for the light-soaked and light + neutron irradiated cells shown in Fig. 3(a and b) highlight the non-reversibility of the neutron-induced effects, while the characteristics before and after light-soaking are virtually identical. If we analyze the device parameters and diode characteristics (Fig. 2(c)), we see that the minimal loss in the PCE after light + neutron (14%) can be mostly attributed to the reduction in the FF (20%) that, in turn, can be related to the large increase/decrease of the series and shunt resistance, respectively. We propose that the worsening of these parameters originates from irreversible neutron-induced traps in the active layer. Of course, alternative possible degradation pathways involving other device elements (*i.e.* the Al/PCBM^{38–41} interface) and/or modification of the collection ability of the ITO electrode due to the large epithermal neutron (10^{-6} – 10^{-1} MeV) absorption cross-section of indium⁴² cannot be ruled out completely. In particular, given the relatively high flux of epithermal neutrons at the

VESUVIO beamline facility ($3.3 \times 10^6 \text{ n cm}^{-2} \text{ s}^{-1}$) the latter scenario would deserve further investigations, and this would be the aim of future experiments at the large-scale facility.

Despite these detrimental effects, the J_{sc} does not report any significant decrease (3%) and V_{oc} shows a 6% increase, a phenomenon linked to the large and unexpected I_0 decrease (40%) that mitigates the worsening of the resistor parameters upon neutron irradiation. This is interesting in the view of possible applications of perovskites in space, as such devices can thus withstand a total fast neutron fluence of $1.5 \times 10^9 \text{ n cm}^{-2}$ featuring only 14% loss in efficiency. The dark current characteristics before and after irradiation (Fig. 3(d and e)) confirm the reversibility of the light-induced damage and the permanent decrease of the leakage current induced by neutrons. In this scenario, we preliminarily attribute the reversible light-induced degradation to the formation of deep-traps that act as recombination centers.^{7,11,37} On the other hand, fast neutrons likely induce permanent defects within the perovskite layer, which would explain the worsening of both series and shunt resistance and, hence, of the fill factor. In the latter case, we speculate that fast neutrons would be able to cause atomic displacement and, given the disparity in the ion size in such materials, can lead to the formation of Frenkel defects (pair of vacancies and interstitials) as happens for inorganic semiconductors.⁴³ These would be shallow traps exhibiting energies close to the valence or conduction band owing to the ionic bond nature of perovskite,^{44,45} which act as unintentional dopants that contribute to the decrease of I_0 . Note that a similar effect has been recently found for proton bombarded perovskite PVs.¹² In addition, as it has been pointed



out in the previous paragraph, epithermal neutron absorption of indium in the electron-collecting electrode might also contribute to the overall degradation pathway. This might also explain the higher PCE loss of the neutron irradiated devices in this study which is also related to the worsening of the resistor parameters (14% with 1.5×10^9 fast neutrons cm^{-2} and 8×10^{10} epithermal neutrons cm^{-2}) compared to the proton bombarded ones (no degradation with 2×10^{11} protons cm^{-2}),^{11,12} although direct comparison among these experiments can be difficult due to the different radiation forms,⁴⁶ spectra and protocols. It is also worth reporting a recent experiment in which organic and perovskite solar cells were launched into the stratosphere. Here the authors also observed a marked fill factor drop for perovskite devices, an effect that, however, the authors linked essentially to some encapsulation failure and not to possible degradation of the electrodes.⁴

Conclusions

In summary, we have reported the first *in operando* neutron irradiation experiment on perovskite solar cells. The principal result here is that fast neutron irradiation leads to the formation of permanent defects likely originating from atomic displacement in the active layer, in stark contrast to the reversible light-induced effects. In addition, we speculate that atomic displacement can promote the formation of shallow-traps (likely Frenkel defects) that act as dopants, and contribute to the decrease of the leakage current. Although further investigations (*i.e.* spectroscopic) are needed to gain more details on the origin of such effects, our findings demonstrate that perovskite PVs can be highly resilient against one of the most hazardous forms of radiation, and hold promise for effective employment in space and avionic applications.

Conflicts of interest

There are no conflicts to declare.

Acknowledgements

We acknowledge the financial support from the EU Horizon 2020 Research and Innovation Programme under Grant No. 643238 (SYNCHRONICS). This work was also supported by the EU FP7 Marie Curie Initial Training Network CONTEST. G.M.P. was supported by an IMPACT PhD studentship co-sponsored by UCL and ISIS-Neutron and Muon Facility (Science and Technology Facilities Council). F.C. is a Royal Society Wolfson Foundation Research Merit Award holder.

References

- W. Zhang, G. E. Eperon and H. J. Snaith, *Nat. Energy*, 2016, **1**, 16048.
- G. E. Eperon, G. M. Paternò, R. J. Sutton, A. Zampetti, A. A. Haghighirad, F. Cacialli and H. J. Snaith, *J. Mater. Chem. A*, 2015, **3**, 19688–19695.
- M. Kaltenbrunner, G. Adam, E. D. Glowacki, M. Drack, R. Schwödiauer, L. Leonat, D. H. Apaydin, H. Groiss, M. C. Scharber, M. S. White, N. S. Sariciftci and S. Bauer, *Nat. Mater.*, 2015, **14**, 1032–1039.
- I. Cardinaletti, T. Vangerven, S. Nagels, R. Cornelissen, D. Schreurs, J. Hruby, J. Vodnik, D. Devisscher, J. Kesters, J. D'Haen, A. Franquet, V. Spampinato, T. Conard, W. Maes, W. Deferme and J. V. Manca, *Sol. Energy Mater. Sol. Cells*, 2018, **182**, 121–127.
- NASA - Printable Spacecraft, https://www.nasa.gov/directorates/spacetech/niac/short_printable_spacecraft.html, accessed 2 January 2019.
- J. M. Ball and A. Petrozza, *Nat. Energy*, 2016, **1**, 16149.
- D. Meggiolaro, S. G. Motti, E. Mosconi, A. J. Barker, J. Ball, C. Andrea Riccardo Perini, F. Deschler, A. Petrozza and F. De Angelis, *Energy Environ. Sci.*, 2018, **11**, 702–713.
- G. M. Paternò, N. Mishra, A. J. Barker, Z. Dang, G. Lanzani, L. Manna and A. Petrozza, *Adv. Funct. Mater.*, 2018, **1805299**, 1805299.
- F. Lang, O. Shargaieva, V. V. Brus, H. C. Neitzert, J. Rappich and N. H. Nickel, *Adv. Mater.*, 2018, **30**, 1702905.
- N. Klein-Kedem, D. Cahen and G. Hodes, *Acc. Chem. Res.*, 2016, **49**, 347–354.
- F. Lang, N. H. Nickel, J. Bundesmann, S. Seidel, A. Denker, S. Albrecht, V. V. Brus, J. Rappich, B. Rech, G. Landi and H. C. Neitzert, *Adv. Mater.*, 2016, **28**, 8726–8731.
- V. V. Brus, F. Lang, J. Bundesmann, S. Seidel, A. Denker, B. Rech, G. Landi, H. C. Neitzert, J. Rappich and N. H. Nickel, *Adv. Electron. Mater.*, 2017, **3**, 1600438.
- Y. Miyazawa, M. Ikegami, H.-W. Chen, T. Ohshima, M. Imaizumi, K. Hirose and T. Miyasaka, *iScience*, 2018, **2**, 148–155.
- T. W. Armstrong and B. L. Colborn, *Radiat. Meas.*, 2001, **33**, 229–234.
- K. Yajima, H. Yasuda, M. Takada, T. Sato, T. Goka, H. Matsumoto and T. Nakamura, *J. Nucl. Sci. Technol.*, 2010, **47**, 31–39.
- P. Goldhagen, J. M. Clem and J. W. Wilson, *Adv. Space Res.*, 2003, **32**, 35–40.
- J. F. Ziegler and W. A. Lanford, *Science*, 1979, **206**, 776–788.
- J. F. Ziegler and W. A. Lanford, *J. Appl. Phys.*, 1981, **52**, 4305–4312.
- T. J. O'Gorman, J. M. Ross, A. H. Taber, J. F. Ziegler, H. P. Muhlfeld, C. J. Montrose, H. W. Curtis and J. L. Walsh, *IBM J. Res. Dev.*, 1996, **40**, 41–50.
- G. Paternò, F. Cacialli and V. García-Sakai, *Chem. Phys.*, 2013, **427**, 142–146.
- G. M. Paternò, J. R. Stewart, A. Wildes, F. Cacialli and V. G. Sakai, *Polymer*, 2016, **105**, 407–413.
- C. Andreani, R. Senesi, A. Paccagnella, M. Bagatin, S. Gerardin, C. Cazzaniga, C. D. Frost, P. Picozza, G. Gorini, R. Mancini and M. Sarno, *AIP Adv.*, 2018, **8**, 8–13.
- G. M. Paternò, V. Robbiano, K. J. Fraser, C. Frost, V. García Sakai and F. Cacialli, *Sci. Rep.*, 2017, **7**, 41013.
- R. Bedogni, A. Esposito, C. Andreani, R. Senesi, M. P. De Pascale, P. Picozza, A. Pietropaolo, G. Gorini, C. D. Frost



- and S. Ansell, *Nucl. Instrum. Methods Phys. Res., Sect. A*, 2009, **612**, 143–148.
- 25 C. Andreani, M. Krzystyniak, G. Romanelli, R. Senesi and F. Fernandez-Alonso, *Adv. Phys.*, 2017, **66**, 1–73.
 - 26 C. Andreani, A. Pietropaolo, A. Salsano, G. Gorini, M. Tardocchi, A. Paccagnella, S. Gerardin, C. D. Frost, S. Ansell and S. P. Platt, *Appl. Phys. Lett.*, 2008, **92**, 114101.
 - 27 R. F. Miller, *Atl. Geol.*, 1990, **26**, 97–107.
 - 28 H. S. Kim, I. H. Jang, N. Ahn, M. Choi, A. Guerrero, J. Bisquert and N. G. Park, *J. Phys. Chem. Lett.*, 2015, **6**, 4633–4639.
 - 29 V. Robbiano, G. M. Paternò, G. F. Cotella, T. Fiore, M. Dianetti, M. Scopelliti, F. Brunetti, B. Pignataro and F. Cacialli, *J. Mater. Chem. C*, 2018, **6**, 2502–2508.
 - 30 G. M. Paternò, M. W. A. Skoda, R. Dalgliesh, F. Cacialli and V. García Sakai, *Sci. Rep.*, 2016, **6**, 34609.
 - 31 <https://www.ossila.com/pages/perovskite-solar-cells-fabrication-guide-using-i101-perovskite-precursor-ink>, <https://www.ossila.com/pages/perovskite-solar-cells-fabrication-guide-using-i101-perovskite-precursor-ink>, accessed 3 January 2019.
 - 32 A. Zampetti, PhD dissertation, University of Rome Tor Vergata, 2014.
 - 33 N. S. J. Kennedy, R. Eastell, C. M. Ferrington, J. D. Simpson, M. A. Smith, J. A. Strong and P. Tothill, *Phys. Med. Biol.*, 1982, **27**, 697–707.
 - 34 J. Shi, J. Dong, S. Lv, Y. Xu, L. Zhu, J. Xiao, X. Xu, H. Wu, D. Li, Y. Luo and Q. Meng, *Appl. Phys. Lett.*, 2014, **104**, 063901.
 - 35 K. Miyano, N. Tripathi, M. Yanagida and Y. Shirai, *Acc. Chem. Res.*, 2016, **49**, 303–310.
 - 36 A. Cuevas, *Energy Procedia*, 2014, **55**, 53–62.
 - 37 W. Nie, J. C. Blancon, A. J. Neukirch, K. Appavoo, H. Tsai, M. Chhowalla, M. A. Alam, M. Y. Sfeir, C. Katan, J. Even, S. Tretiak, J. J. Crochet, G. Gupta and A. D. Mohite, *Nat. Commun.*, 2016, **7**, 11574.
 - 38 S. H. Yoo, J. M. Kum and S. O. Cho, *Nanoscale Res. Lett.*, 2011, **6**, 1–7.
 - 39 G. Paternò, A. J. Warren, J. Spencer, G. Evans, V. G. Sakai, J. Blumberger and F. Cacialli, *J. Mater. Chem. C*, 2013, **1**, 5619–5623.
 - 40 G. Tregnago, M. Wykes, G. M. Paternò, D. Beljonne and F. Cacialli, *J. Phys. Chem. C*, 2015, **119**, 11846–11851.
 - 41 G. M. Lazzerini, G. M. Paternò, G. Tregnago, N. Treat, N. Stingelin, A. Yacoot and F. Cacialli, *Appl. Phys. Lett.*, 2016, **108**, 053303.
 - 42 J. Dawidowski, J. R. Granada, J. R. Santisteban, F. Cantargi and L. A. R. Palomino, *Exp. Methods Phys. Sci.*, 2013, **44**, 471–528.
 - 43 G. H. Kinchin and R. S. Pease, *Rep. Prog. Phys.*, 1955, **18**, 1–51.
 - 44 E. Mosconi, D. Meggiolaro, H. J. Snaith, S. D. Stranks and F. De Angelis, *Energy Environ. Sci.*, 2016, **9**, 3180–3187.
 - 45 W.-J. Yin, T. Shi and Y. Yan, *Appl. Phys. Lett.*, 2014, **104**, 063903.
 - 46 A. Ruzin, G. Casse, M. Glaser, A. Zanet, F. Lemeilleur and S. Watts, *IEEE Trans. Nucl. Sci.*, 1999, **46**, 1310–1313.

